Novel Two-dimensional Carbon Allotrope with Strong Electronic Anisotropy

Cong Su,[1,2] Hua Jiang,[1] and Ji Feng[1,*]

[1] *International Center for Quantum Materials, Peking University, Beijing 100871, China*
[2] *Yuanpei College, Peking University, Beijing 100871, China*

Two novel two-dimensional carbon allotropes comprised of octagons and pentagons are proposed based on the first-principle calculations. The two carbon allotropes, named OPG-L and OPG-Z, are found to have distinct properties. OPG-L is metallic, while OPG-Z is a gapless semimetal. Remarkably, OPG-Z exhibits pronounced electronic anisotropy with highly anisotropic Dirac points at the Fermi level. A tight-binding model is suggested to describe the low-energy quasiparticles, which clarifies the origin of the anisotropic Dirac points. Such an anisotropic electronic characteristic of OPG-Z is expected to have wide implications in nano-electronics.

PACS numbers: 61.48. Gh, 61.46.-w, 68.65.-k

There have been growing interests in exploring new structures of the two-dimensional (2D) carbon in recent years. This is primarily stimulated by extensive investigations on the intriguing properties of graphene [1], an atomically thin semimetal that harbors Dirac fermions at a pair of inequivalent valleys in the **k**-space [2]. Among others, graphyne [3], graphdiyne [4], graphane [5], the sp^2-like carbon layer with five-, six- and seven-membered rings [6], the 2D amorphous carbon with four-membered rings [7], the planar carbon pentaheptite [8], the 2D carbon semiconductor with patterned defects [9], several carbon networks [10], octagraphene [11] and T graphene [12] have been studied theoretically. In a clever synthetic attempt, graphdiyne has been successfully prepared experimentally [4]. One-dimensional (1D) topological defect containing octagonal and pentagonal sp^2-hybridized carbon rings embedded in a perfect graphene has been produced experimentally [13]. The result is a line defect that mimics the 1D metallic wire, which has potential application in all-carbon valleytronics [14, 15]. Consequently, one naturally suspects that the other 2D metastable carbon allotropes with intriguing properties may be prepared, in particular, comprised of five- and eight-membered carbon rings as inspired by the line defect in graphene.

Apparently, viewing the line defects as structural motifs whose tiling covers the 2D plane is a sensible pathway for discovering new stable 2D carbon allotropes. Indeed, such tilings are geometrically viable. In this work, a 2D carbon allotrope is suggested to have an intrinsic strong electronic anisotropy, without the need for an external field [16]. By using the first-principles calculations, we propose two novel energetically competitive, kinetically stable 2D carbon allotropes. They can be viewed as 2D tessellations of octagons and pentagons, called OP graphene-L (OPG-L) and OPG-Z, as shown in Figs. 1(a) and (b), respectively. The structure of OPG-L can be viewed as juxtaposing the five-five-eight-membered rings (558) ribbon (indicated by the red atoms in Fig. 1) along a straight line path, while the OPG-Z along a zigzag path, as indicated by the green arrows in Figs. 1 (a) and (b). It is worth noting that this 558 ribbon occurs experimentally as a topological line defect of graphene [13]. By calculating the energy dispersions, we show that the OPG-L is a metal and OPG-Z is a gapless semimetal. Analysis of the electronic structures reveal that OPG-Z displays a strong electronic anisotropy, with anisotropic Dirac points near the Fermi level. These novel 2D carbon structures, with the proposed electronic properties, may be useful for novel electronic applications, in particular in all-carbon electronics [17].

Our calculations are based on the density functional theory (DFT) within the generalized gradient approximation (GGA), in the form of Perdew-Burke-Ernzerhof's exchange-correlation functional [18]. All the calculations are performed using the Vienna Ab-initio Simulation

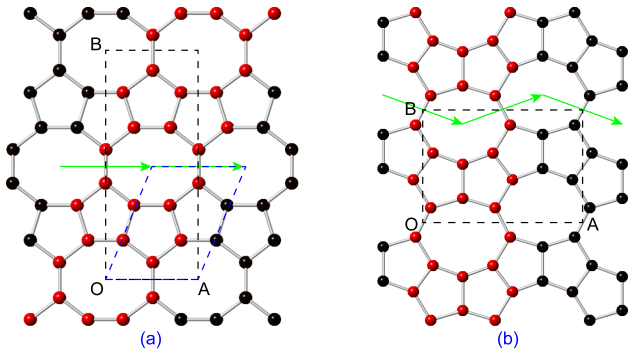

FIG. 1: The structures of (a) OPG-L and (b) OPG-Z (space group *Pmma*). The black dashed frames are the orthogonal unit cells of OPG-L and OPG-Z, where OA and OB are lattice vectors. These two structures can be tiled by the red-colored 558 structure by copying it along the green arrows. The primitive cell of OPG-L is shown in blue dashed frame while the primitive cell of OPG-Z is the same as the crystal cell. Here we give the structural information of unit cells from the DFT calculations. OPG-L: space group *Cmmm*, OA = 3.68 Å, OB = 9.12 Å, two atoms in the asymmetric unit cell, (0, 0.42) and (0.69, 0.33); OPG-Z: space group *Pmma*, OA = 6.90 Å, OB = 4.87 Å, four atoms in asymmetric unit cell, (0.45,0.87), (0.56,0.62), (0.25,0.48), (0.25,0.78).

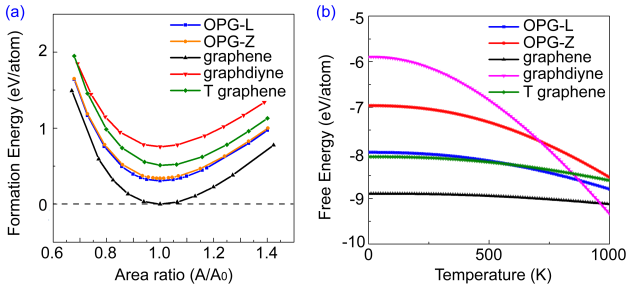

FIG. 2: (a) The formation energies of OPG-L, OPG-Z, graphdiyne and T graphene as a function of area ratio in comparison to graphene, where A_0 is the optimized lattice area. The formation energy of graphene is set to 0. (b) The Helmholtz free energy as a function of temperature for the above-mentioned 2D carbon allotropes.

Package (VASP) [19]. Periodic boundary conditions were employed and vacuum slabs of 10 Å were used to isolate the replicated OPG layers. Geometrical optimizations are performed until the Hellmann-Feynman forces on the ions are less than 1.0×10^{-4} eV/Å. The plane-wave basis is used, with a cut-off that converges the total energy to 1 meV/atom. The Brillouin zone is sampled using $9 \times 9 \times 1$ Monkhorst-Pack **k**-point scheme [20]. The phonon spectra are calculated using the finite-displacement method in a $3 \times 3 \times 1$ supercell [21].

In order to gauge the stability of the proposed carbon structures, we calculated the formation energies, at $T = 0$ K within the static lattice approximation, of OPG-L, OPG-Z, and three other typical 2D carbon allotropes, namely graphene, graphdiyne [4] and T graphene [12] for comparison [Fig. 2(a)]. The formation energy of defined with respect to the free-standing graphene monolayer. Among all the structures, graphene is the most stable energetically, in agreement with the results in the previous work [22]. It is found that OPG-L and OPG-Z have fairly close formation energies, 0.31 eV/atom and 0.34 eV/atom respectively. Therefore, OPG-L and OPG-Z are energetically metastable compared with graphene, though much stabler than previously proposed T graphene [12] (whose formation energy is 0.52 eV/atom) and graphdiyne [4] (0.76 eV/atom). It should be noted that the successful synthesis of graphdiyne in a previous work [4] implies the realization of OPG-L and OPG-Z is not unlikely.

We further estimated the Helmholtz free energy as a function of temperature T. The Helmholtz free energy $A(T)$ is approximated as:

$$A(T) \approx A_{ph}(T) + E(0) \qquad (1)$$

where $A_{ph}(T)$ is the vibrational free energy within the Born-Oppenheimer approximation, and $E(0)$ is the total static-lattice energy at 0 K. The finite-temperature Fermi-Dirac distribution of electronic level occupation and the electron-phonon coupling are neglected. The vibrational free energy is calculated by $A_{ph}(T) = \frac{1}{2}\sum_{\mathbf{q},s}\hbar\omega(\mathbf{q},s) + k_BT\sum_{\mathbf{q},s}\ln[1-exp(-\hbar\omega(\mathbf{q},s)/k_BT)]$, where $\mathbf{q}$ stands for the wavevector, s the branch index, ω the frequency, k_B and $\hbar$ the Boltzmann and Planck's constants, respectively. As a result, we find that the free energy of OPG-L and OPG-Z [Fig. 2(b)] falls rapidly with increasing temperature. The difference between OPG-L and graphene is reduced greatly when temperature approaches 1000 K. To further examine the kinetic stability, the phonon spectra of OPG-L and OPG-Z are calculated (see supplementary material, Fig. S1). No imaginary phonon modes are found, confirming again the kinetic stability of these two carbon sheets. In addition, the chemical stability of these two structures are also examined. We put dioxygen and dihydrogen molecules close to OPG-L and OPG-Z. After geometric relaxations, these molecules are all repelled by the carbon sheet. Therefore, no spontaneous chemical reaction is expected between these structures and oxygen or hydrogen molecules, suggesting their redox stability in atmosphere.

The Kohn-Sham electronic band structures and density of states (DOS) of OPG-L and -Z are shown in Fig. 3. As we can see, OPG-L is a metal and OPG-Z is a gapless semimetal. In Fig. 3(c), Γ =(0,0) point (fractional coordinates with respect to the reciprocal unit cell; we follow

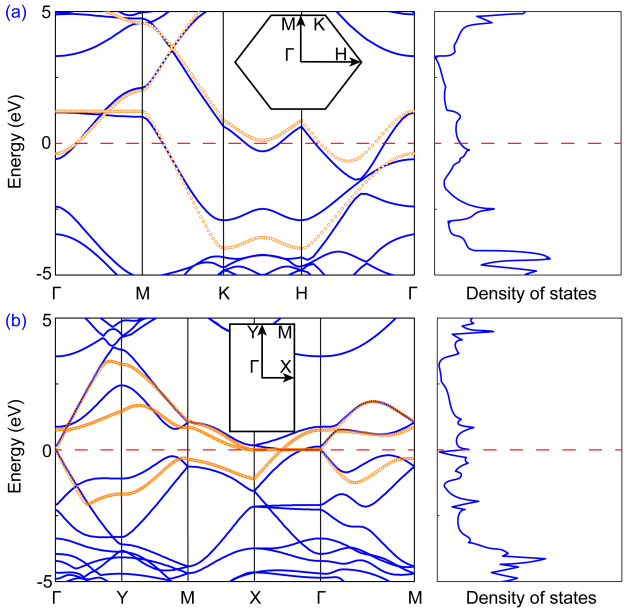

FIG. 3: Electronic band structures and density of states of OPG-L and -Z: (a) The energy dispersion and DOS for OPG-L; (b) The BS and DOS for OPG-Z. The inset figures are locations of high symmetry points. The red dashed lines represent Fermi levels, which are set to 0 eV. Blue lines are the results of DFT calculations, while orange dotted lines are the results of tight-binding model.

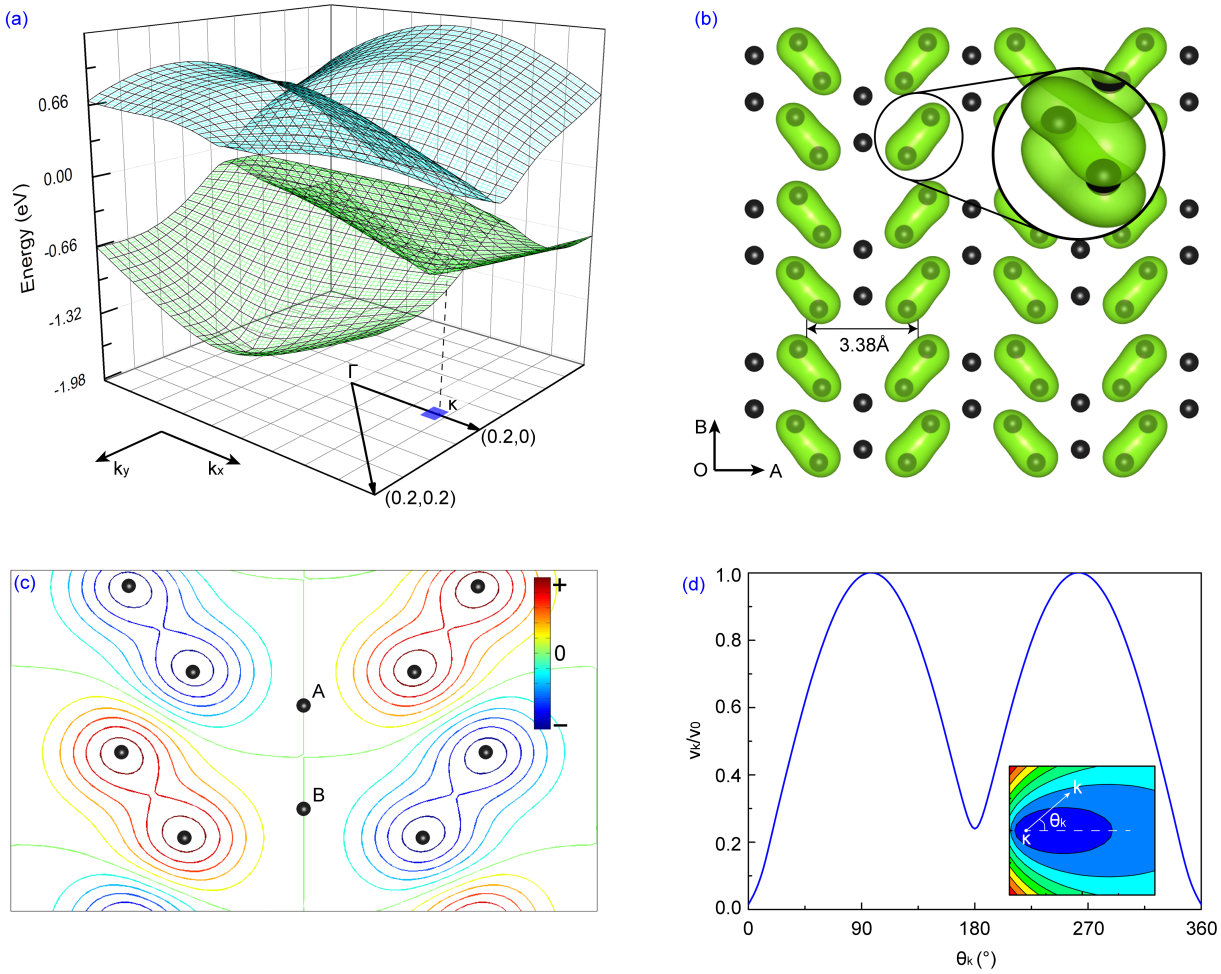

FIG. 4: (a) The blow-up band structures of Kohn-Sham quasiparticles of OPG-Z near the Fermi level around Γ point. (b) The partial charge density (PCD) at κ point near Fermi level, calculated by DFT. (c) The wave function in a unit cell at the same point, calculated by the tight-binding model [Eq.(1)]. (d) The component of group velocity parallel to the $\mathbf{k}$ vector (v_k) measured from the κ point in units of the Fermi velocity along k_y (v_0) versus the angle (θ_k) of the $\mathbf{k}$ vector. Inset: The isosurface of OPG-Z within the range of $k_x \in [0.139, 0.141]$ and $k_y \in [-0.0001, 0.0001]$. The black dots in (b) and (c) are carbon atoms.

the same notation hereafter) near the Fermi level (FL) is dominated by linear dispersion, resembling the Dirac fermions. A closer inspection reveals that OPG-Z has a wedge-shaped conduction band and valence band near the FL where the Dirac points emerge at $\kappa = (0.139, 0)$ and $\kappa' = (-0.139, 0)$, as shown in Fig. 4(a). The Fermi velocity along k_y at these Dirac points are estimated to be 2.2×10^5 m/s, relatively high but an order of magnitude smaller than in pristine graphene. The Kohn-Sham quasiparticle energy isosurfaces of conduction band of OPG-Z near κ point are very elongated ellipses with an eccentricity near unity [inset of Fig. 4(d)]. In addition, the Fermi velocities along different directions measured from κ point are also calculated [Fig. 4(d)], which shows that the group velocity is redueced to 3.2×10^3 m/s in the k_x direction. Therefore, OPG-Z is semimetallic with highly anisotropic Dirac fermions [16].

To further understand the DFT calculated results, we construct a tight-binding model of OPG-Z by allowing for the electrons hopping only to nearest neighbors. The Hamiltonian can be written as [23]

$$H = -\sum_{\langle i,j\rangle\sigma} t_{ij}(a^\dagger_{i\sigma}a_{j\sigma} + h.c.) + \varepsilon_0 \sum_{i,\sigma} a^\dagger_{i\sigma}a_{i\sigma}, \qquad (2)$$

where $a^\dagger_{i\sigma}$ is the creation operator of an electron with spin σ of the carbon valence p_z orbital at site i; $\langle i,j\rangle$ stands for the nearest-neighbor pairs of atoms at site i and site j; ε_0 is the on-site energy and t_{ij} are the hopping matrix elements between site i and site j, which are all taken to be 3.0 eV [24] except for t_{AB} [1 eV, site A and site B are shown in Fig. 4(c)]. Because all the atoms in our two

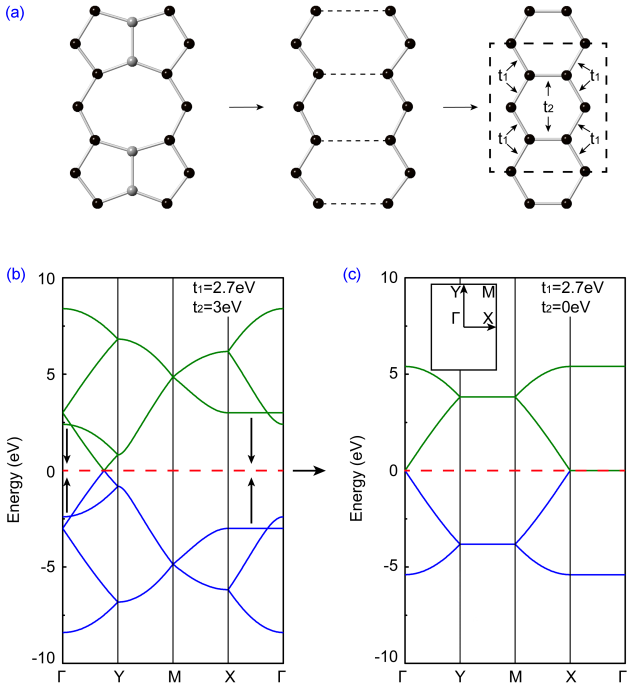

FIG. 5: (a) The transfer process from OPG-Z to graphene. Gray atoms are the atoms with zero charge density around Fermi level in OPG-Z. The supercell of graphene consists of eight atoms with its TB hopping matrix elements t_1 and t_2 are shown. (b) The tight-binding band structure of graphene in the supercell shown in (a), with $t_2 = 3eV$. (c) The TB band structure of graphene of the same primitive cell, with $t_2 = 0eV$. Inset: high symmetry points of the graphene supercell.

structures are carbons, we can simply set the on-site energy to zero. We calculated the band structures (orange dotted lines in Fig. 3), which are observed to match well the DFT calculations. The partial charge density at κ point in the conduction band is also calculated by DFT, shown in Fig. 4(b), which is in excellent agreement with the wavefunction calculated by the TB [Fig. 4(c)]. Notice that the nodes of the wavefunction locate at the same sites with atoms A and B in Fig. 4(c). In this case, the electron density is zero on these atoms, naturally splitting the whole plane into independent 1D electron channels along OB direction [Fig. 4(b)]. It is this continuity of electron density along OB and the strong localization of electrons along OA that brings about the anisotropic electronic conductivity in OPG-Z. In this case, a perfect 1D aligned electron transport is able to be realised in OPG-Z. Such stripe-like electron transport channels are as wide as 3.38 Å [Fig. 4(b)]. The anisotropic property of electronic transport in OPG-Z may give rise to some interesting implications in nano-electronics. For example, the 1D electronic channels in OPG-Z layer can be a replacement of the conducting wires in thin film transistor.

It is also worth mentioning how the Dirac points and flat band emerge around FL in OPG-Z. Since the elimination of the zero-charge-density atom pairs simply creates a distorted graphene layer [Fig. 5(a)], a TB model of graphene would be good to describe some of the OPG-Z's properties. By expanding the primitive cell of graphene to eight-atom supercell, two linear dispersion bands and flat bands at $E = \pm t_2$ are folded to the Γ point in the first Brillouin zone [Fig. 5(b)]. With decreasing t_2 to zero, these two sets of band are translated to FL, creating one linear dispersion and one flat band at Γ point [Fig. 5(c)]. As can be seen, the anisotropic property of OPG-Z is originated from the separation of zigzag ribbons in graphene. The spliting of Dirac point from Γ point in this model to κ and κ' points in OPG-Z occurs from the symmetry-breaking of the bond lengths in each zigzag ribbon (see supplementary material, Fig. S3).

Owing to its formation energy and free energy lower than the existing carbon allotropes like graphdiyne [4], OPG-Z might be experimentally obtained. One procedure might be the newly emerged nano-engineering method [25–27], while on the other hand, it would be a choice that by taking advantage of the standard methods for graphene production on substrates like SiC [28] or Cu [29, 30], one may as well find a substrate suitable for epitaxial or CVD method to produce the new carbon allotropes of OPG-L and OPG-Z. In addition, the acetylene scaffolding ways [31] to synthesize segments of OPG-L and OPG-Z, say the successfully synthesized planar dicyclopenta pentalene [32], may be also possible.

In summary, by means of the first-principle calculations we have predicted two new 2D carbon allotropes comprised of octagons and pentagons, named as OPG-L and OPG-Z. The energetic and kinetic stabilities of OPG-L and -Z are checked and their electronic structures are calculated. Our results show that OPG-L and OPG-Z are even more favorable in energy than graphdiyne that was already synthesized experimentally. OPG-L is a metal while OPG-Z is a gapless semimetal. It is found that OPG-Z possesses an amazing anisotropic electronic property as well as two anisotropic Dirac points in its first Brillouin zone. The wave function and partial charge density in the conduction band of OPG-Z at κ point indicate that the 1D electronic transport can be realised in OPG-Z, which may give rise to some implications in nano-electronics. Additional calculations are carried out to explain the origin of this anisotropy.

We are grateful to Ran Duan and Dr. Haiwen Liu for useful discussions. We thank the financial support from National Science Foundation of China (Grant No. 11174009, No. 91121004) and China 973 Project (Grant No. 2013CB921900).

* Electronic address: jfeng11@pku.edu.cn

[1] K. S. Novoselov, A. K.Geim, S. V. Morozov, D. Jiang, M. I. Katsnelson, I. V. Grigorieva, S. V. Dubonos, and A. A. Firsov, Nature (London) **438**, 197 (2005).

[2] P.R. Wallace, Phys. Rev. **71**, 622 (1947).

[3] M. M. Haley, Pure Appl. Chem. **80**, 519 (2008); J. M. Kehoe *et al.*, Org. Lett. **2**, 969 (2000).

[4] G. X. Li, Y. L. Li, H. B. Liu, Y. B. Guo, Y. J. Li and D. B. Zhu, Chem. Commun. **46**, 3256 (2010).

[5] J. O. Sofo, A. S. Chaudhari, and G. D. Barber, Phys. Rev. B **75**, 153401 (2007); D. C. Elias *et al.*, Science **323**, 610 (2009).

[6] H. Terrones, M. Terrones, E. Hernández, N. Grobert, J-C. Charlier, and P. M. Ajayan, Phys. Rev. Lett. **84**, 1716 (2000).

[7] J. Kotakoski, A.V. Krasheninnikov, U. Kaiser, and J. C. Meyer, Phys. Rev. Lett. **106**, 105505 (2011).

[8] V. H. Crespi, L. X. Benedict, M. L. Cohen, and S. G. Louie, Phys. Rev. B **53**, R13303 (1996).

[9] David J. Appelhans, Zhibin Lin, and Mark T. Lusk, Phys. Rev. B **82**, 073410 (2010).

[10] A.N. Enyashin and A.L. Ivanovskii, Phys. Status Solidi B **248**, 1879 (2011).

[11] X. L. Sheng, H. J. Cui, F. Ye, Q. B. Yan, Q. R. Zheng, and G. Su, J. Appl. Phys. **112**, 074315 (2012).

[12] Y. Liu, G. Wang, Q. S. Huang, L. W. Guo and X. L. Chen, Phys. Rev. Lett. **108**, 225505 (2012).

[13] Jayeeta Lahiri, You Lin, Pinar Bozkurt, Ivan I. Oleynik, and Matthias Batzill, Nature Nanotech. **5**, 326 (2010).

[14] D. Gunlycke, C. T. White, Phys. Rev. Lett. **106**, 136806 (2011).

[15] J. T. Song, H. W. Liu, H. Jiang, Q. -F. Sun and X. C. Xie, Phys. Rev. B **86**, 085437 (2012).

[16] C. -H. Park, L. Yang, Y. -W. Son, M. L. Cohen, and S. G. Louie, Nature Phys. **4**, 213 (2008).

[17] A. Das, S. Pisana, B. Chakraborty, S. Piscanec, S. K. Saha, U. V. Waghmare, K. S. Novoselov, H. R. Krishnamurthy, A. K. Geim, A. C. Ferrari and A. K. Sood, Nature Nanotech. **3**, 210 (2008).

[18] J.P. Perdew, K. Burke and M. Ernzerhof, Phys. Rev. Lett. **77**, 3865 (1996).

[19] G. Kresse and J. Furthmüller, Phys. Rev. B **54**, 11169 (1996).

[20] H.J. Monkhorst and J.D. Pack, Phys. Rev. B **13**, 5188 (1976).

[21] A. Togo, F. Oba and I. Tanaka, Phys. Rev. B **78**, 134106 (2008).

[22] X. L. Sheng, Q. B. Yan, F. Ye, Q. R. Zheng and G. Su, Phys. Rev. Lett. **106**, 155703 (2011).

[23] S. Chakravarty, Condensed Matter Physics (lecture notes, 2011).

[24] A. H. Castro Neto, F. Guinea, N. M. R. Peres, K. S. Noselov and A. K. Geim, Rev. Mod. Phys. **81**, 109 (2009).

[25] A. Hashimoto, K. Suenaga, A. Gloter, K. Urita and S. Iijima, Nature (London) **430**, 870 (2004).

[26] S. Okada, T. Kawai and K. Nakada, J. Phys. Soc. Jpn. **80**, 013709 (2011).

[27] M. T. Lusk and L. D. Carr, Phys. Rev. Lett. **100**, 175503 (2008).

[28] J. Hass, W.A. Heer and E.H. Conrad, J. Phys.: Condens. Mater. **20**, 323202 (2008).

[29] X. S. Li, W. W. Cai, J. An, S. Kim, J. Nah, D. X. Y, R. Piner, A. Velamakanni, I. Jung, E. Tutuc, S. K. Banerjee, L. Colombo and R. S. Ruoff, Science **324**, 1312 (2009).

[30] A. Reina, X. T. Jia, J. Ho, D. Nezich, H. Son, V. Bulovic, M. S. Dresselhaus and J. Kong, Nano Letters **9**, 30 (2009).

[31] S. W. Slayden and J. F. Liebman, Chem. Rev. **101**, 1541 (2001); U. H. F. Bunz, Y. Rubin and Y. Tobe, Chem. Soc. Rev. **28**, 107 (1999).

[32] H. Cao, S. G. V. Ornum, J. Deschamps, J. F.-Anderson, F. Laib and J. M. Cook, J. Am. Chem. Soc. **127**, 933 (2005).